POLITECNICO DI TORINO
Repository ISTITUZIONALE

Experimental Evaluation of Energy Degradation of Photovoltaic Plants after 20+ Operation Years

*Original*
Experimental Evaluation of Energy Degradation of Photovoltaic Plants after 20+ Operation Years / Malgaroli, G., Schubert, S., Matturro, F., Ciocia, A., Cocina, V., Di Leo, P., Spertino, F.. - ELETTRONICO. - (2024), pp. 1-6. (2024 9th International Youth Conference on Energy (IYCE) Colmar (France) 02-06 July 2024) [10.1109/IYCE60333.2024.10634954].

*Availability:*
This version is available at: 11583/2997558 since: 2025-02-17T13:52:16Z

*Publisher:*
IEEE

*Published*
DOI:10.1109/IYCE60333.2024.10634954

*Terms of use:*

This article is made available under terms and conditions as specified in the corresponding bibliographic description in the repository

*Publisher copyright*
IEEE postprint/Author's Accepted Manuscript

©2024 IEEE. Personal use of this material is permitted. Permission from IEEE must be obtained for all other uses, in any current or future media, including reprinting/republishing this material for advertising or promotional purposes, creating new collecting works, for resale or lists, or reuse of any copyrighted component of this work in other works.

(Article begins on next page)

28 November 2026

# Experimental Evaluation of Energy Degradation of Photovoltaic Plants after 20+ Operation Years

1st Gabriele Malgaroli *Dip. Energia "Galileo Ferraris"*
*Politecnico di Torino*
Torino, Italy
gabriele.malgaroli@polito.it 2nd Stefano Schubert *Dip. Energia "Galileo Ferraris"*
*Politecnico di Torino*
Torino, Italy
stefano.schubert@polito.it 3rd Fabiana Matturro *Dip. Energia "Galileo Ferraris"*
*Politecnico di Torino*
Torino, Italy
fabiana.matturro@studenti.polito.it 4th Alessandro Ciocia *Dip. Energia "Galileo Ferraris"*
*Politecnico di Torino*
Torino, Italy
alessandro.ciocia@polito.it 5th Valeria Cocina *Dip. Energia "Galileo Ferraris"*
*Politecnico di Torino*
Torino, Italy
valeria.cocina@polito.it 6th Paolo Di Leo *Dip. Energia "Galileo Ferraris"*
*Politecnico di Torino*
Torino, Italy
paolo.dileo@polito.it 7th Filippo Spertino *Dip. Energia "Galileo Ferraris"*
*Politecnico di Torino*
Torino, Italy
filippo.spertino@polito.it

**Abstract**

In the context of the ever-growing importance of renewable energy sources, the long-term reliability assessment of PhotoVoltaic (PV) systems emerges as a critical aspect of ensuring sustainable energy production with cost-effective technologies. Nowadays, the first PV plants, installed at early 2000s, have achieved more than 20 years of operation: this reflects their predicted lifetime. Hence, evaluating their efficiency at the end of the estimated lifetime can provide important information regarding the real performance in accordance with the manufacturers' declaration. Actually, this study evaluates the performance of two PV arrays, installed at early 2000s at the university campus of Politecnico di Torino (Turin, Italy, latitude = 45° N), characterised by monocrystalline silicon (m-Si) modules and different inverters configurations. In particular, all the modules of the PV plants were tested under natural sunlight, and their performances were corrected to Standard Test Conditions (STC), according to the International Standards. This work estimated the measured power deviations, which were compared to the quantities predicted by the manufacturers after these operation years, and the average yearly degradation rates. The results revealed that the minimum performances guaranteed by the manufacturers of the modules (yearly degradation rate of about -0.8%) are satisfied, with only a few exceptions. Finally, a visual inspection was carried out to identify visible defects among the modules.

*Keywords—renewable energy systems, performance, efficiency, photovoltaic module array, degradation.*

## I. Introduction

In the pursuit of improving the Renewable Energy Sources (RESs) exploitation, solar PhotoVoltaic (PV) plants and wind farms are the most efficient technologies. One of the research fields in the renewable sector consists of the accurate estimation of RES performance over time. Regarding wind farms, the focus of this line of research is on their performance assessment with respect to manufacturer declaration [1]. On the contrary, one of the main aspects the PV research is currently focusing on is the development of advanced models to accurately predict PV production and contribute to fault detection [2]. This paper contributes to these efforts by focusing on the development of an automated diagnostic method for PV plants by the inverters. Current diagnostic approaches in this field typically involve traditional tests such as infrared thermography or electroluminescence [3]. These methods, however, are costly, especially for large-scale PV plants that often require drones [4], and do not facilitate continuous monitoring of plant health. In order to correctly estimate PV production and perform an efficient diagnosis, the degradation of the systems needs to be taken into account. Actually, the performance and the reliability of PV technology degrade over time due to many factors including environmental stresses, material degradation, manufacturing defects, system

failures and others [5], [6]. Nowadays, degradation in multi-MW plants can be investigated also adopting more sophisticated technologies like drones to detect faults or failures in the systems [7]. It is clear that, in this context, the cost-effectiveness of PV systems is strongly affected by their degradation rate: hence, monitoring and quantifying this aspect of each PV plant is fundamental to correctly predict the energy yield and the economic returns of the investment [8]. In literature, many works estimate the power reduction of PV systems with respect to initial specifications at Standard Test Conditions (STC) [9], which can be due to many physical phenomena such as encapsulant discoloration, solder bond fatigue, delamination, interconnect failures, frame damage, glass and cell breakage, Potential-Induced Degradation (PID) and others. In addition, other factors like weather conditions [10], [11] or design choices (e.g., the inverters configuration) might significantly affect the performance of PV plants over time [12], [13]. The measurement of PV power reduction with respect to STC can be performed using a variety of approaches and equipment, either in situ (e.g., under natural sunlight) or under controlled conditions (e.g., under artificial sunlight). For these procedures, generally, the equipment includes current-voltage (*I-V*) curve tracers, solar radiation sensors and temperature sensors [9]. Moreover, the PV power reduction of a PV module can be estimated through different models (empirical, analytical or numerical), which include factors like temperature, irradiance, solar spectrum, shading, mismatch and others [14].

In the paper [15], the authors examined the rate of degradation of 22 distinct photovoltaic power plants located across four continents. Thirteen of these installations consist of moncrystalline silicon (m-Si) PV modules that have been in operation for a maximum of twenty-five years, showing a degradation rate that falls in a range between 0.7% and 3.19% per year. On the other hand, the remaining installations use different technology or are not covered by the standard warranty anymore (25 years).

This paper aims to quantify the power degradation of two PV plants (rated power of 1 and 1.5 kW) with monocrystalline silicon (m-Si) modules, different inverters configuration and about 20 operation years. In particular, in the present work, the performance for the modules of the plants under study were tested under natural sunlight and corrected to Standard Test Conditions (STC) according to the International Standards. Finally, the yearly degradation rate of each module was quantified and compared with their manufacturer declaration. The paper is structured as follows: Section II describes the different inverters configurations for PV plants, and Section III presents the PV systems under analysis. Section IV describes the measurement setup adopted to acquire the most important electrical quantities from the plants, while Section V shows the results of the study. Finally, the conclusions of this work are included in Section VI.

## II. Inverters configurations in PV plants

The configurations of DC/AC converters of a PV plant can be of three types: central, string or multi-string, and AC modules [16].

### A. Central inverters

In the centralized technology, DC/AC converters interface a large number of PV modules to the grid [17] to increase the rated voltage of the inverter. This inverter configuration is, typically, characterised by a rated power ranging between 500 kW to a few MW for medium to large power plants. In such a configuration, many PV strings, each consisting of series-connected modules, are connected in parallel in a combiner box, and their cumulative production is sent to a central inverter. Alternatively, inverters are defined as centralized when they interface arrays with high ratios between array power and the total power of the system. In utility scale installations, with many MW of rated power, this configuration is preferred due to the ability of central inverters in managing higher installed power. Moreover, their higher reliability and lower cost with respect to smaller converters make them even more advantageous to adopt. However, the main drawback of central inverters is their vulnerability to failures and underperformance: actually, even a single fault or underperformance in the part of the plant connected to the central inverter, e.g. due to mismatch, shading or other events, affects the total production of the converter [18], [19]. Indeed, in this condition multiple peaks originate in the power-voltage ($P$-$V$) curve of the generator, and the maximum power point tracking might fail in identifying the maximum power point, resulting in noticeable energy losses. Under such conditions, systems with central inverters exhibit decreased efficiency and power output as the performance of the entire system is impacted by the lowest performing modules, especially on cloudy or partially shaded days [20].

For this reason, conventional techniques of tracking are preferred due to their simplicity when the local peaks of the $P-V$ curve are a few. Examples of such techniques are the perturb and observe, hill climbing method, incremental conductance, the load current/load voltage, and maximization open circuit voltage methodology.

### B. String inverters

Currently, string inverters are the most common configuration for grid-connected PV plants: they have a much lower capacity than a central inverter, and each string of the PV array is connected to a different inverter [21]. In this case, the maximum power point tracking is performed at string level, achieving lower energy losses due to *I-V*curve mismatch rather than central inverters. This configuration is preferred for residential installations with rated power up to about 10 kW thanks to their modularity and

cost-effectiveness. In addition, as mismatch conditions due to partial shading occur in such systems, local maximum power points generally arise in the power-voltage ($P-V$) curve and the tracking of the global maximum might be complex. In these conditions, conventional algorithms might fail and other more complex techniques are preferred as biologically inspired optimization techniques based on deterministic particle swarm optimization [22], colony of foraging ants [23], and flashing fireflies [24].

In order to overcome the rated power of string inverters, the multi-string inverter configuration can be adopted. In this case, the inverters are equipped with a maximum power tracker for each string, limiting the mismatch losses among the different strings of the array [25].

### C. Micro-inverters

In the micro-inverters, or "AC modules", configuration, one converter is built into each PV module, or is located underneath [26]. As one inverter is integrated in each module, its operation is not affected by that of other modules in the PV plants, avoiding losses due to the mismatch among the PV modules. Moreover, micro-inverters have second class insulation (class II) against direct and indirect contacts; no grounding is required, and the system reliability is higher than other typologies thanks to the lower number of components. Microinverters ensure that each module operates independently, significantly improving system performance in various environmental conditions, including partial shading, thereby maintaining optimal power output even if some modules are underperforming [20]. However, this solution is expensive, and, generally, micro-inverters are used with modules having an output power up to about 300 W.

## III. Plants under analysis

The plants under study are two PV systems (Fig. 1), with m-Si modules, installed at the university campus of Politecnico di Torino (Turin, Italy, latitude = 45° N) at early 2000s. They are South oriented (azimuth = 0°) and have a tilt angle of 30° and 25° for PV plants #1 and #2, respectively.

The first system (PV plant #1) was installed in 2000 and is powered by 18 PV modules manufactured by the company BP Solar (rated power of 1.5 kW). The modules are grouped in two strings of 9 modules each, and the plant has one central inverter with rated power of 1.5 kW and DC/AC conversion efficiency of 93%. The second plant (PV plant #2) was installed in 2003 and includes 10 modules manufactured by the company Isofotón (rated power of 1 kW). Moreover, each module integrates one inverter located on its rear side (micro-inverter or AC modules configuration), with rated power of 100 W and conversion efficiency = 94%. Table I reports the main specifications for the PV modules of the two plants.

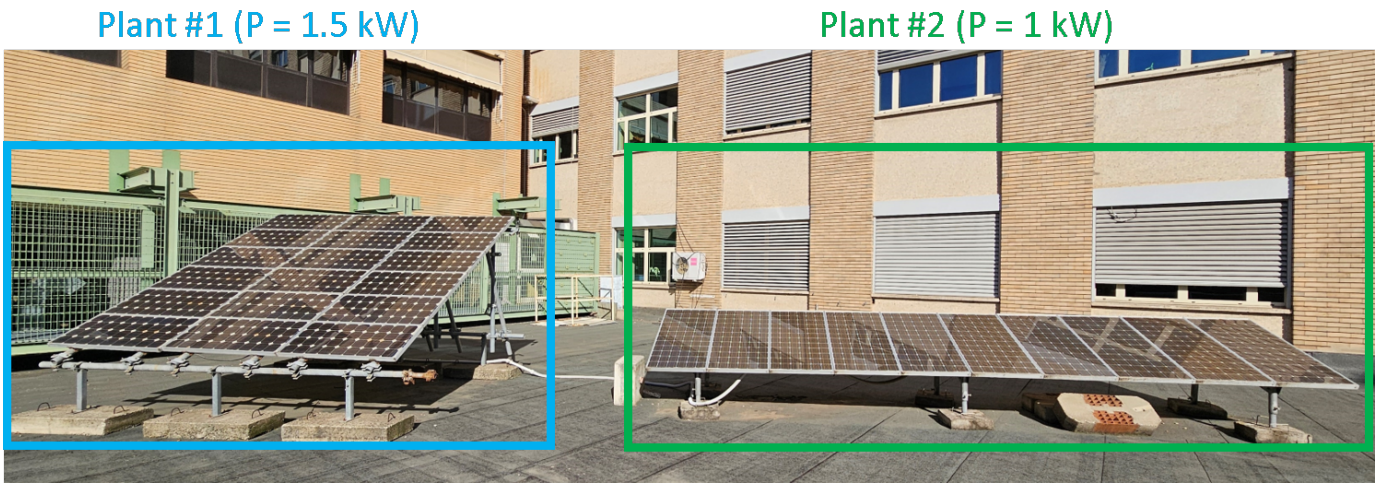


Fig. 1. PV plants under study.

## IV. Measurement system

The measurement system used to acquire experimental data is based on the transient charging of a capacitive load, in which one capacitor is initially discharged, and it is supplied by the PV module under test. The capacitor charging is controlled by a power breaker that, after the closing of the circuit, permits the PV generator to supply the capacitive load from the short-circuit to the open-circuit condition. As, generally, current peaks may occur in the short-circuit and such data need to be removed from the analysis, a negative pre-charge is applied to the capacitor to improve the quality of the data. As the duration of the charging transient $t$ is affected by the capacitance of the capacitive load, the latter is selected in order to obtain desired values

TABLE I
SPECIFICATIONS OF THE PV MODULES UNDER STUDY

| Manufacturer | BP Solar | Isofotón |
|---|---|---|
| Model | BP585 | I-110/24 |
| Rated power $P_m$ (W) | 85 | 110 |
| MPP current $I_m$ (A) | 4.7 | 3.16 |
| MPP voltage $V_m$ (V) | 18 | 34.8 |
| Short-circuit current $I_{sc}$ (A) | 5 | 3.38 |
| Open-circuit voltage $V_{oc}$ (V) | 22.1 | 43.2 |
| Thermal coefficient for $I_{sc}$ (%/°C) | 0.065 | 0.04 |
| Thermal coefficient for $V_{oc}$ (%/°C) | -0.36 | -0.367 |
| Thermal coefficient for $P_m$ (%/°C) | -0.5 | -0.45 |
| NOCT (°C) | 47 | 44.6 |

of transient duration. The paper [27] reports the dependency of the capacitance on the short-circuit current $I_{sc}$, the open-circuit voltage $V_{oc}$, the number of parallel-connected PV strings $N_p$, and the number of PV modules in series per string $N_s$. In this work, a capacitance of 10 mF is selected to obtain transient durations lower than 300 ms with irradiance at Standard Test Conditions (STC), corresponding to solar irradiance of $1000\ \mathrm{W/m^2}$ and modules' temperature of $25°\mathrm{C}$.

In this measurement system, the *I-V*curves of the PV modules are acquired with an Automatic Data Acquisition System (ADAS) to store simultaneously the irradiance $G$, the air temperature $T_a$, and the PV current and voltage. The ADAS is periodically calibrated and it consists of the following components [28]:

- A notebook PC with a LabVIEW software emulating a digital storage oscilloscope.
- A multifunction data acquisition board with one A/D converter (successive approximation technology, 16 bit-resolution, sampling rate up to 1.25 MSa/s, maximum input of $\pm$10 V, internal amplifier gains for lower ranges) and multiplexer.
- A differential voltage probe with two attenuation ratios 20:1 and 200:1 for voltage levels up to 140 V and 1400 V, respectively.
- Two current probes (Hall effect) with an output sensitivity of 100 mV/A for current values up to $\pm$30 A, one for current measurement and the other one for trigger source.
- A secondary standard pyranometer acquires irradiance with uncertainty $< \pm 2\%$.
- A thermometer to acquire ambient temperature.
- A temperature probe to acquire the temperature on the rear side of the module.
- A capacitive load with capacitance equal to 10 mF.

The schematic of the measurement circuit is shown in Figure 2.

## V. RESULTS

The performance related to the modules constituting the PV plants of this study were tested under natural sunlight in 2022 (solar irradiance $>$ 900 W/m$^2$) with the measurement system described in Section IV. In particular, three *I-V*curves were measured for each PV module in a time interval of about 250 ms with a sampling rate of 50 kHz. Then, the acquired voltage and current signals were corrected to Standard Test Conditions (STC, with $G_{STC}$ = 1000 W/m$^2$ and $T_{STC}$ = 25°C) according to the standards, and the average values of each module were obtained. The equations provided by the standards are the following, in which the subscript "m" refers to measurement conditions [29]:

$$I_{STC} = I_m + I_{sc,m} \cdot \left( \frac{G_{STC}}{G_m} - 1 \right) + \alpha \cdot (T_{STC} - T_m) \tag{1}$$

$$V_{STC} = V_m - R_{s,m} \cdot (I_{STC} - I_m) - k \cdot I_{STC} \cdot (T_{STC} - T_m) + \beta \cdot (T_{STC} - T_m) \tag{2}$$

The quantities of the equation are the following:

- $I_{STC}$ is the current at STC conditions (A).
- $I_m$ is the measured current (A).
- $I_{sc,m}$ is the measured short circuit current (A).
- $V_{STC}$ is the voltage at STC conditions (V).
- $V_m$ is the measured voltage (V).
- $R_{s,m}$ is the series resistance of the module ($\Omega$).
- $G_m$ is the measured irradiance (W/m$^2$).
- $T_m$ is the measured temperature (°C).
- $\alpha$ is the thermal coefficient of current (%/°C).
- $\beta$ is the thermal coefficient of voltage (%/°C).
- $k$ is a correction parameter (-).

Tables II and III report the main results of the analysis for PV plant #1 and #2, respectively: for each module, the relative deviations with respect to the manufacturer specifications in terms of power ($\Delta P$), voltage ($\Delta V_{mpp}$), and current ($\Delta I_{mpp}$) are

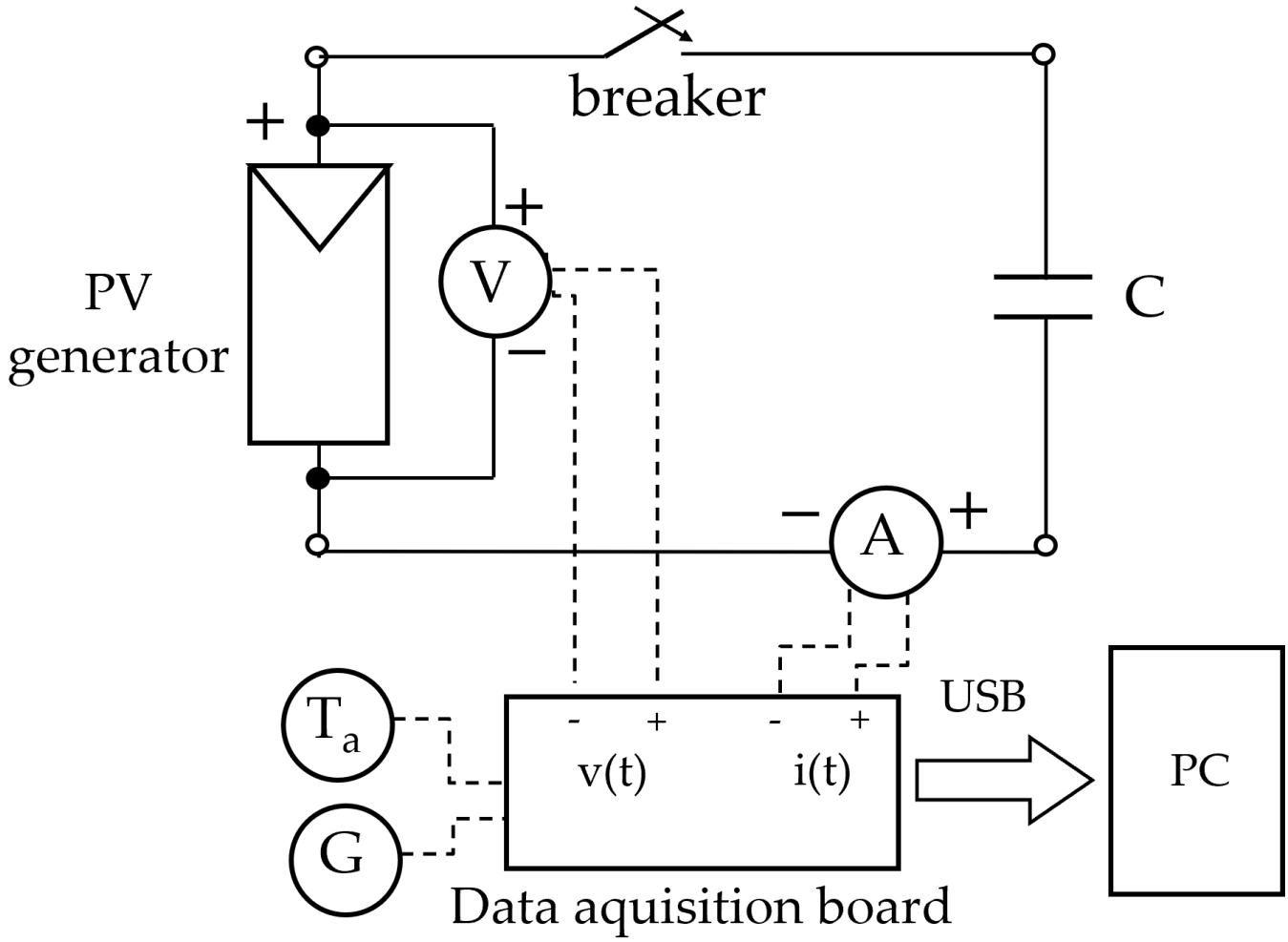


Fig. 2. Schematic of the measurement circuit.

listed, as well as the efficiency $\eta$ and the yearly degradation rate $r$, which is the ratio between $\Delta P$ and the number of operation years.

Almost half of the modules in PV plant #1 (7 out of 18, corresponding to about 40 % of the generators) meet the maximum degradation rate guaranteed for PV systems designed at early 2000s. Indeed, the majority of commercial PV modules were guaranteed to provide about 80% of rated performance after 25 years, corresponding to a yearly degradation rate of about -0.8%. [30]. In this plant, the worst yearly degradation rate occurs for PV module 5B ($r$ = -1.04%, with a power reduction of about -24%), while module 3B has the best performance as it exhibits a power loss of about -13%, and a degradation rate of about -0.6%.

Regarding PV plant #2, the module with the worst performance has a power reduction of about -26%, corresponding to a yearly degradation rate of about -1.4%; on the contrary, the best performance occurs for a module with a power reduction of about -14% and a degradation rate of about -0.7%. In this system, only 20 % of the generators meet the maximum degradation rate declared by the manufacturer. Moreover, for all the modules of the two plants, most of performance loss is due to current reduction rather than to voltage reduction. Thus, the average yearly degradation rate is evaluated for both the systems, being -0.86%/y and -0.97%/y for PV plants #1 and #2, respectively, corresponding to an average power reduction of -18.9% and -18.4%. These values are 7.5% and 21% higher than manufacturer indications: actually, in both systems, most of PV modules do not meet the maximum degradation rate requirement of -0.8%/y. The lowest degradation rate occurs for the plant equipped with PV modules including solar cells with larger active area (square with side length of 5 and 4 inches for modules of plants #1 and #2, respectively) and, thus, manufactured with greater wafers.

In addition, a visual inspection was carried out for the modules under test, and figures 3 and 4 show a PV module from plant #1 and #2, respectively. As it is possible to see, the modules are affected by defects. In particular, the most frequent one is given by discoloration, or ”browning” of the encapsulating layer (Ethylene-Vinyl Acetate, EVA) in the regions closer to the busbars, i.e., with the highest modules’ temperature. This defect is more evident for modules of PV plant #2; moreover, mechanical cracks affect a few cells, and noticeable dirt increases the power reduction of the modules.

TABLE II
MEASUREMENTS UNDER NATURAL SUNLIGHT FOR PV PLANT #1

| Mod. ID | $P_{mpp}$ | $\Delta P$ | $\Delta I$ | $\Delta V$ | $\eta$ | $r$ |
|---|---|---|---|---|---|---|
| 1A | 70.6 W | -16.9% | -13.1% | -5.82% | 11.1% | -0.73%/y |
| 1B | 70.5 W | -17.1% | -15.7% | -3.14% | 11.1% | -0.74%/y |
| 1C | 71.6 W | -15.7% | -14.1% | -3.42% | 11.3% | -0.68%/y |
| 2A | 66.4 W | -21.8% | -15.8% | -8.61% | 10.5% | -0.95%/y |
| 2B | 69.1 W | -18.7% | -18.2% | -2.11% | 10.9% | -0.81%/y |
| 2C | 68.5 W | -19.4% | -15.7% | -5.86% | 10.8% | -0.84%/y |
| 3A | 71.8 W | -15.5% | -14.1% | -3.12% | 11.3% | -0.67%/y |
| 3B | 73.6 W | -13.4% | -13.7% | -1.22% | 11.6% | -0.58%/y |
| 3C | 67.2 W | -21.0% | -16.7% | -6.47% | 10.6% | -0.95%/y |
| 4A | 71.2 W | -16.2% | -15.8% | -2.07% | 11.2% | -0.71%/y |
| 4B | 71.3 W | -16.1% | -14.4% | -3.49% | 11.2% | -0.70%/y |
| 4C | 68.3 W | -19.7% | -17.9% | -3.67% | 10.7% | -0.85%/y |
| 5A | 68.5 W | -19.4% | -16.6% | -4.77% | 10.8% | -0.84%/y |
| 5B | 64.6 W | -23.9% | -20.7% | -5.58% | 10.2% | -1.04%/y |
| 5C | 67.4 W | -20.7% | -17.0% | -5.85% | 10.6% | -0.90%/y |
| 6A | 65.1 W | -23.4% | -21.8% | -3.59% | 10.2% | -1.02%/y |
| 6B | 67.5 W | -20.5% | -15.3% | -7.58% | 10.6% | -0.89%/y |
| 6C | 66.9 W | -21.3% | -20.6% | -2.38% | 10.5% | -0.92%/y |

TABLE III
MEASUREMENTS UNDER NATURAL SUNLIGHT FOR PV PLANT #2

| Mod. ID | $P_{mpp}$ | $\Delta P$ | $\Delta I$ | $\Delta V$ | $\eta$ | $r$ |
|---|---|---|---|---|---|---|
| 1 | 85.3 W | -22.5% | -18.3% | -5.10% | 9.95% | -1.18%/y |
| 2 | 81.2 W | -26.2% | -18.2% | -9.72% | 9.47% | -1.38%/y |
| 3 | 88.9 W | -19.2% | -17.8% | -1.61% | 10.4% | -1.01%/y |
| 4 | 89.1 W | -19.0% | -16.6% | -2.79% | 10.4% | -1.00%/y |
| 5 | 94.4 W | -14.1% | -13.5% | -0.73% | 11.0% | -0.74%/y |
| 6 | 90.3 W | -17.9% | -17.0% | -1.05% | 10.5% | -0.94%/y |
| 7 | 92.7 W | -15.7% | -13.5% | -2.54% | 10.8% | -0.83%/y |
| 8 | 89.6 W | -18.5% | -16.2% | -2.77% | 10.5% | -0.97%/y |
| 9 | 94.1 W | -14.5% | -14.0% | -0.57% | 11.0% | -0.76%/y |
| 10 | 92.0 W | -16.3% | -15.3% | -1.22% | 10.7% | -0.86%/y |

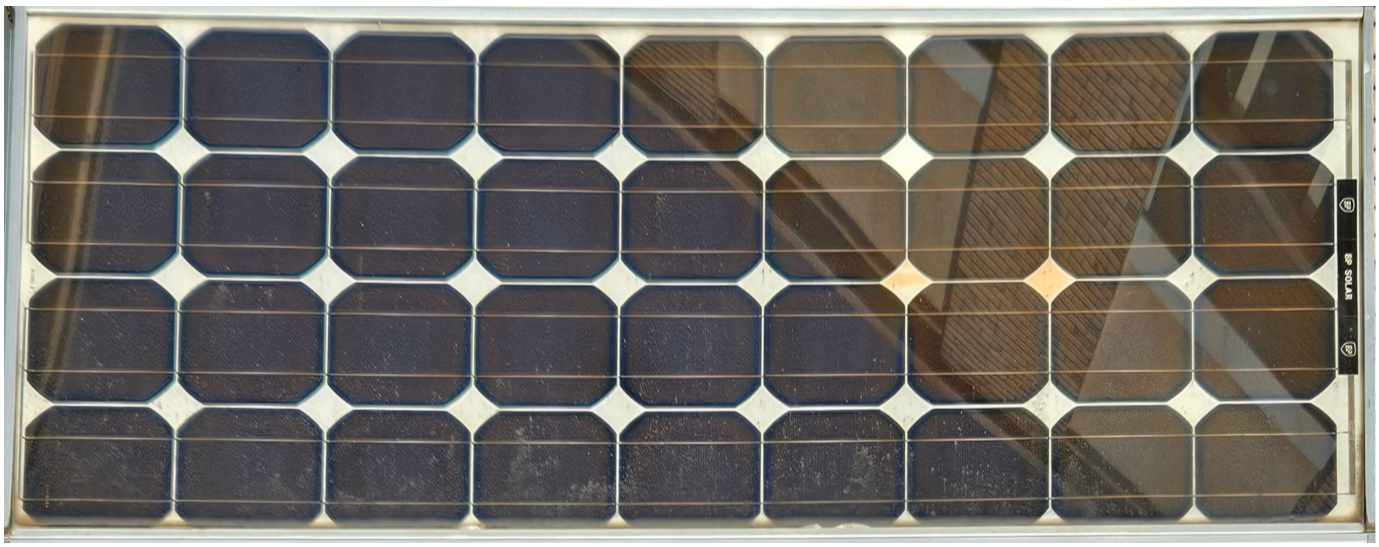


Fig. 3. Focus on one PV module from plant #1.

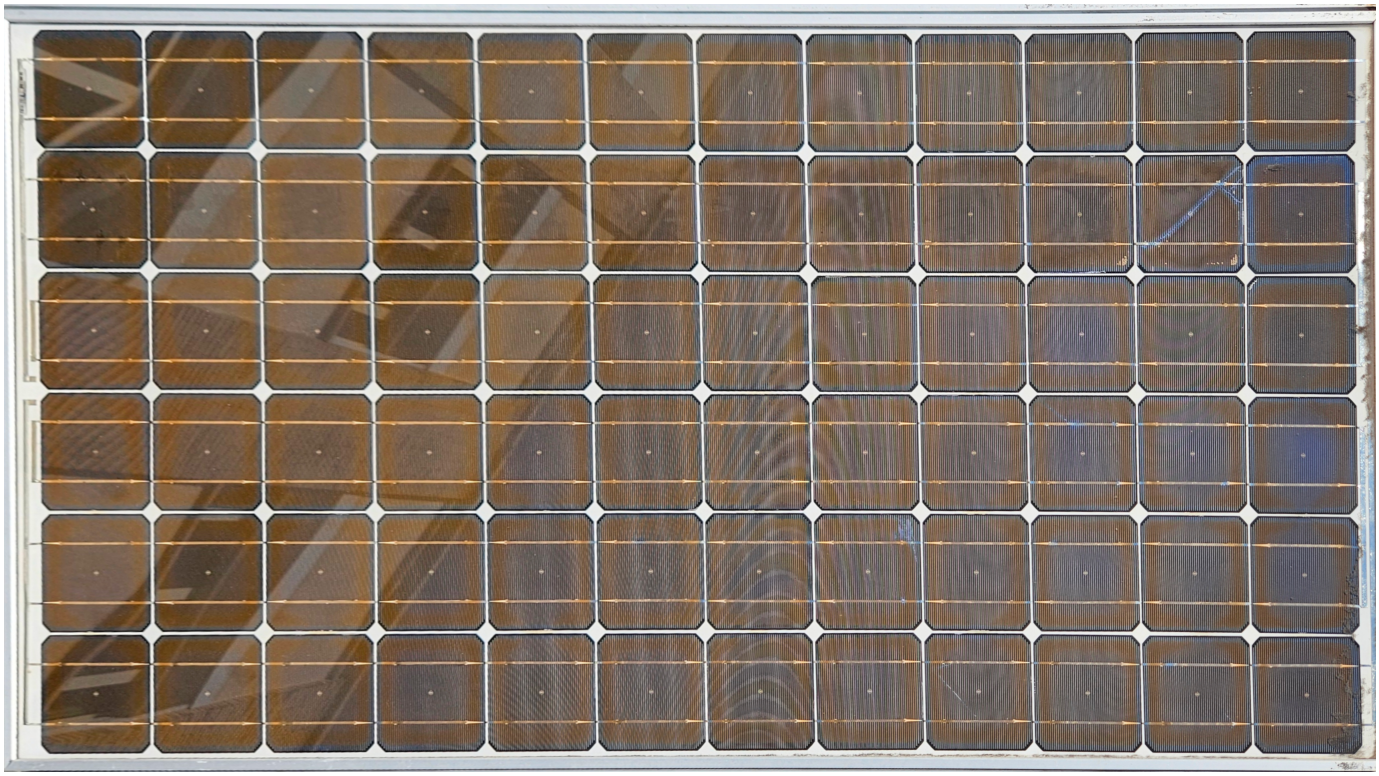

Fig. 4. Focus on one PV module from plant #2.

## VI. Conclusions

The lifetime of Photovoltaic (PV) generators might be strongly affected by degradation, providing a huge effect on its cost-effectiveness and performances. In particular, even if the lifetime of new PV installations is expected to reach about 40 years, however, this prediction is not valid for old plants, whose lifetime was up to 20-30 years. This paper evaluates the average yearly power degradation of two PV plants, with monocrystalline silicon modules installed and a rated power of a few kW for both. The plants, installed at the university campus of Politecnico di Torino (Turin, Italy, latitude = 45° N), are equipped with central inverter (plant #1) and micro-inverters (plant #2). The performance of the modules was determined under natural sunlight in 2022 and, then, corrected to Standard Test Conditions (STC) according to the International Standards. The average yearly degradation rate was -0.86%/y and -0.97%/y for PV plants #1 and #2, respectively, corresponding to an average power reduction of 18.9% and 18.4%. The lowest degradation rate occurs for the plant with the central inverter configuration (plant #1); however, for both the systems, the results for most of PV modules do not meet the minimum performance guaranteed by the manufacturers at early 2000s (yearly degradation rate of about -0.8%). Hence, future works developing automatic fault detection algorithms will need to take into account a tolerance regarding the real degradation rate of PV systems. Such a tolerance is recommended to be of about 10% for modules with cells of 4 inches-sides, and about 20% for modules with cells of 5 inches-sides.

## References


[1] A. Carullo, A. Ciocia, P. Di Leo, F. Giordano, G. Malgaroli, L. Peraga, F. Spertino, and A. Vallan, "Comparison of correction methods of wind speed for performance evaluation of wind turbines," 2020, p. 291 – 296.

[2] F. Spertino, G. Malgaroli, A. Amato, M. Qureshi, A. Ciocia, and H. Siddiqi, "An innovative technique for energy assessment of a highly efficient photovoltaic module," *Solar*, vol. 2, 2022.

[3] A. Ciocia, A. Carullo, P. DI Leo, G. Malgaroli, and F. Spertino, "Realization and Use of an IR Camera for Laboratory and On-field Electroluminescence Inspections of Silicon Photovoltaic Modules." Institute of Electrical and Electronics Engineers Inc., 2019.

[4] F. Bizzarri, S. Nitti, and G. Malgaroli, "The use of drones in the maintenance of photovoltaic fields," *E3S Web of Conferences*, vol. 119, p. 21, 2019.

[5] S. Begum, R. Banu, G. F. Ahammed, B. D. Parameshachari, and Rajashekarappa, "Performance degradation issues of pv solar power plant," *International Conference on Electrical, Electronics, Communication Computer Technologies and Optimization Techniques, ICEECCOT 2017*, vol. 2018-January, pp. 311–313, 7 2017.

[6] A. Sinha, S. Pore, A. Balasubramaniyan, and G. S. T. Mani, "Acceleration factor modeling for degradation rate prediction of photovoltaic encapsulant discoloration," *2018 IEEE 7th World Conference on Photovoltaic Energy Conversion, WCPEC 2018 - A Joint Conference of 45th IEEE PVSC, 28th PVSEC and 34th EU PVSEC*, pp. 1342–1346, 11 2018.

[7] F. Bizzarri, S. Nitti, and G. Malgaroli, "The use of drones in the maintenance of photovoltaic fields," *E3S Web of Conferences*, vol. 119, p. 00021, 9 2019.

[8] J. Cuadrado, E. Martinez, E. Puertas, and J. C. Martinez-Santos, "Long-term effects of degradation on photovoltaic system return on investment," *IEEE Latin America Transactions*, vol. 21, pp. 1282–1290, 12 2023.

[9] J. Walters, H. Seigneur, E. Schneller, M. Matam, and M. Hopwood, "Experimental methods to replicate power loss of pv modules in the field for the purpose of fault detection algorithm development," *Conference Record of the IEEE Photovoltaic Specialists Conference*, pp. 1410–1413, 6 2019.

[10] N. Okada, S. Yamanaka, H. Kawamura, and H. Ohno, "Energy loss of photovoltaic system caused by irradiance and incident angle," *3rd World Conference onPhotovoltaic Energy Conversion, 2003. Proceedings of*, 2003.

[11] C. Libby, B. Paudyal, X. Chen, W. B. Hobbs, D. Fregosi, and A. Jain, "Analysis of pv module power loss and cell crack effects due to accelerated aging tests and field exposure," *IEEE Journal of Photovoltaics*, vol. 13, pp. 165–173, 1 2023.

[12] H. Qamar, H. Qamar, N. Korada, and R. Ayyanar, "Low frequency ripple reduction in input dc current and ac line currents with 240 clamped space vector pwm in grid-connected photovoltaic converters," *IEEE Open Journal of Power Electronics*, vol. 4, pp. 415–426, 2023.

[13] K. Orikawa and J. I. Itoh, "Power loss reduction of a ac-dc converter features 10-v and 10,000-a sintering power supply," *15th International Power Electronics and Motion Control Conference and Exposition, EPE-PEMC 2012 ECCE Europe*, 2012.

[14] Y. Mahmoud, "Power loss estimation approach for pv systems operating under faults," *IECON Proceedings (Industrial Electronics Conference)*, vol. 2022-October, 2022.

[15] D. H. Daher, M. Aghaei, D. A. Quansah, M. S. Adaramola, P. Parvin, and C. Ménézo, "Multi-pronged degradation analysis of a photovoltaic power plant after 9.5 years of operation under hot desert climatic conditions," *Progress in Photovoltaics: Research and Applications*, vol. 31, no. 9, pp. 888–907, 2023. [Online]. Available: https://onlinelibrary.wiley.com/doi/abs/10.1002/pip.3694

[16] F. Spertino, G. Chicco, A. Ciocia, G. Malgaroli, A. Mazza, and A. Russo, "Harmonic distortion and unbalance analysis in multi-inverter photovoltaic systems," *SPEEDAM 2018 - Proceedings: International Symposium on Power Electronics, Electrical Drives, Automation and Motion*, pp. 1031–1036, 8 2018.

[17] S. Deshpande and N. R. Bhasme, "A review of topologies of inverter for grid connected pv systems," in *2017 Innovations in Power and Advanced Computing Technologies (i-PACT)*, 2017, pp. 1–6.

[18] N. Foureaux, A. Machado, E. Silva, I. Pires, J. Brito, and F. B. Cardoso, "Central inverter topology issues in large-scale photovoltaic power plants: Shading and system losses," *2015 IEEE 42nd Photovoltaic Specialist Conference, PVSC 2015*, 12 2015.

[19] C. Bufi, A. Elasser, and M. Agamy, "A system reliability trade-off study for centralized and distributed pv architectures," *2015 IEEE 42nd Photovoltaic Specialist Conference, PVSC 2015*, 12 2015.

[20] D. Pal, H. Koniki, and P. Bajpai, "Central and micro inverters for solar photovoltaic integration in ac grid," pp. 1–6, 2016.

[21] S. Harb, M. Kedia, H. Zhang, and R. S. Balog, "Microinverter and string inverter grid-connected photovoltaic system — a comprehensive study," in *2013 IEEE 39th Photovoltaic Specialists Conference (PVSC)*, 2013, pp. 2885–2890.

[22] K. Ishaque and Z. Salam, "A deterministic particle swarm optimization maximum power point tracker for photovoltaic system under partial shading condition," *IEEE Transactions on Industrial Electronics*, vol. 60, pp. 3195–3206, 2013.

[23] K. Sundareswaran, V. Vigneshkumar, P. Sankar, S. P. Simon, P. S. R. Nayak, and S. Palani, "Development of an improved po algorithm assisted through a colony of foraging ants for mppt in pv system," *IEEE Transactions on Industrial Informatics*, vol. 12, pp. 187–200, 2 2016.

[24] K. Sundareswaran, S. Peddapati, and S. Palani, "Mppt of pv systems under partial shaded conditions through a colony of flashing fireflies," *IEEE Transactions on Energy Conversion*, vol. 29, pp. 463–472, 2014.

[25] K. S. Tey and S. Mekhilef, "Modified incremental conductance algorithm for photovoltaic system under partial shading conditions and load variation," *IEEE Transactions on Industrial Electronics*, vol. 61, pp. 5384–5392, 2014.

[26] S. Strache, R. Wunderlich, and S. Heinen, "A comprehensive, quantitative comparison of inverter architectures for various pv systems, pv cells, and irradiance profiles," *IEEE Transactions on Sustainable Energy*, vol. 5, pp. 813–822, 2014.

[27] F. Spertino, J. Ahmad, A. Ciocia, P. D. Leo, A. F. Murtaza, and M. Chiaberge, "Capacitor charging method for i–v curve tracer and mppt in photovoltaic systems," *Solar Energy*, vol. 119, pp. 461–473, 2015.

[28] A. Ciocia, P. D. Leo, S. Fichera, F. Giordano, G. Malgaroli, and F. Spertino, "A novel procedure to adjust the equivalent circuit parameters of photovoltaic modules under shading," *2020 International Symposium on Power Electronics, Electrical Drives, Automation and Motion, SPEEDAM 2020*, pp. 711–715, 6 2020.

[29] "Photovoltaic devices. Procedures for temperature and irradiance corrections to measured I-V characteristics - BS EN IEC 60891:2021," Standard, Feb. 2022.

[30] A. Phinikarides, N. Kindyni, G. Makrides, and G. E. Georghiou, "Review of photovoltaic degradation rate methodologies," *Renewable and Sustainable Energy Reviews*, vol. 40, pp. 143–152, 2014. [Online]. Available: https://www.sciencedirect.com/science/article/pii/S1364032114006078